APPLICATIONS OF CFD TECHNOLOGY TO THE DESIGN OF AIRCRAFT PROPULSION SYSTEMS

Leonard J. Hebert* and Ralph E. Ponsonby*
Propulsion Research Staff, Boeing Commercial Airplane Group,
Seattle, Washington, U.S.A.

Abstract

Application of computational fluid dynamics (CFD) to propulsion system design has become critically important to improving individual engine component and overall airplane performance at The Boeing Company. The Propulsion Research staff of Boeing Commercial Airplane Group applies CFD techniques as a supplement to or in lieu of testing to optimize the design process and lower developmental cost. This paper presents an overview of the CFD methods currently applied to engineering problems in propulsion system design.

Introduction

Commercial aircraft design is becoming increasingly demanding owing to the competitive nature and rising expense of civil air travel. To remain competitive in the marketplace, it is necessary to continually improve aircraft operational efficiency at reasonable developmental cost. A prime area for improvement is found in the propulsion system and its integration with the airframe.

Propulsion system design has traditionally coupled simplified analyses with expensive and time-intensive experimentation. Improving efficiency over current levels requires insight, beyond that attained by the traditional approach, into the fine details of the flow.

The current maturity of CFD and computer technology make possible such insight by increasing the resolution of the involved physical phenomena. Further, use of CFD streamlines the design process through reduction of experimental testing. Both aspects contribute to lower development cost.

The Boeing Company has invested significant resources in developing this technology in an effort to fully attain these advantages in the design of aircraft. This paper outlines the approach to CFD application taken by the Propulsion Research staff and presents selected examples of propulsion system hardware analysis.

Code Development

The philosophy of CFD application held by Propulsion Research is based on the development and maintenance of a system of computer codes, each capable of accurately describing the physical processes involved in a particular class of problem. The modeling incorporated in these programs covers the spectrum from full potential to Reynolds-averaged Navier-Stokes. This variety of codes allows for cost-effective analysis of most propulsion problems. The particular method used for a given application is detailed in the following sections.

Analysis capability is continually expanded through the acquisition of codes from NASA, universities, and other sources to take advantage of recently developed algorithms and physical models and through internal efforts to create methods that can address present specific needs as well as foreseeable propulsion problems.

In addition to the acquisition and internal development of codes, there exists a parallel effort to validate and apply the codes to problems of practical interest. Proper validation of a code is given paramount importance. This procedure defines the accuracy and boundaries of applicability of the program by comparing fundamental flowfield properties (pressure, velocity, temperature) and integrated performance parameters with experimental data prepared specifically for this purpose. In addition, the numerical efficiency of the code (convergence rate) is assessed and guidelines prepared for the efficient running of the program.

The final phase of new-code development involves the creation of a productive computational package useful in the design environment. This effort is targeted at reducing the time necessary to complete an analysis and at improving output clarity. Examples include automated procedures to transfer lofted geometry from the CAD system into the grid generator and postprocessors to graphically display flow-code solutions. The latter is used extensively as it presents both global and minute solution detail, contributing to comprehension and time effectiveness of the computation.

Design Approach and Applications

The infusion of CFD analysis into the design process has proceeded at a pace commensurate with the evolution of computer technology and with the maturation of numerical algorithms. Today The Boeing Company takes full advantage of CFD in the design of its aircraft. There are several significant advantages to this approach, including—

- Time-efficient development and design of geometric configurations:
  - Accuracy of computational results are sufficient for application to some problems not readily simulated by experiment.
  - Effects of perturbations to the geometry often can be analyzed quickly and much less expensively than by testing.
  - Full-scale data can be generated for many cases at realistic flight conditions, helping to alleviate the need for extrapolation of experimental data.

*Senior Research Engineer

- Direct experimental aid supplied through—
  - Definition of instrumentation positions for data retrieval in areas of interest.
  - A net reduction of testing via extension of and interpolation within the experimental data matrix.
  - Calculation of the effects of interference from test apparatus and the development of correction factors.

The design of some engine components can take full advantage of current CFD capabilities with testing used as a final verification procedure. Other components may require more interaction between analysis and testing depending on the prevailing complexity of the flow.

The following overview covers the analytical methods used in the computation of flowfields about various isolated engine components and about fully integrated configurations.

Subsonic Engine Inlets

Among the primary objectives of subsonic inlet design are minimization of weight and drag associated with the size of the inlet, and minimization of total pressure distortion of the flow at the engine fan face under extreme flight conditions. Initial design lines are set roughly by factors such as engine fan diameter, maximum engine airflow, and acoustic treatment requirements in the diffuser for noise abatement. CFD analysis is then applied to the refinement of inlet lip contours to optimize for angle of attack and crosswind capability and to the shape of the diffuser to maximize pressure recovery.

The analysis is effected using a full 3D, transonic, compressible, potential flow code[1-4] coupled with a 3D boundary-layer code.[5] The potential code uses a multigrid approach to speed convergence and is quite general, finding wide applicability owing to its Cartesian/cylindrical formulation. Figure 1 shows a circumferential plane cut through a coarse cylindrical grid in the region of the inlet hilite.

The design of inlets for new-generation, large, high-bypass-ratio, turbofan engines favors an oblique shape, where the lower quadrants are extended radially outward (fig. 2). This approach satisfies airflow and ground-clearance requirements while minimizing landing gear weight. Measured and calculated (potential only) Mach numbers are compared in figure 2 along a cut drawn 45 deg from the keel line. The discrepancy between analysis and test data in the diffuser is due to the lack of viscous modeling at this stage of the computation.

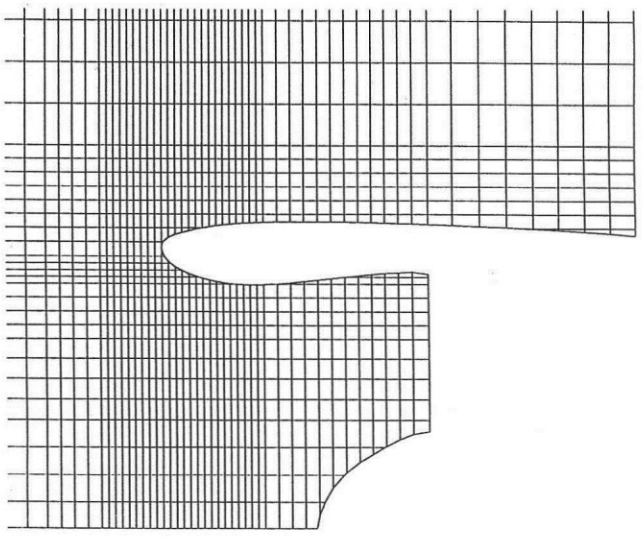

Figure 1. Example of a Computational Grid About a Subsonic Inlet

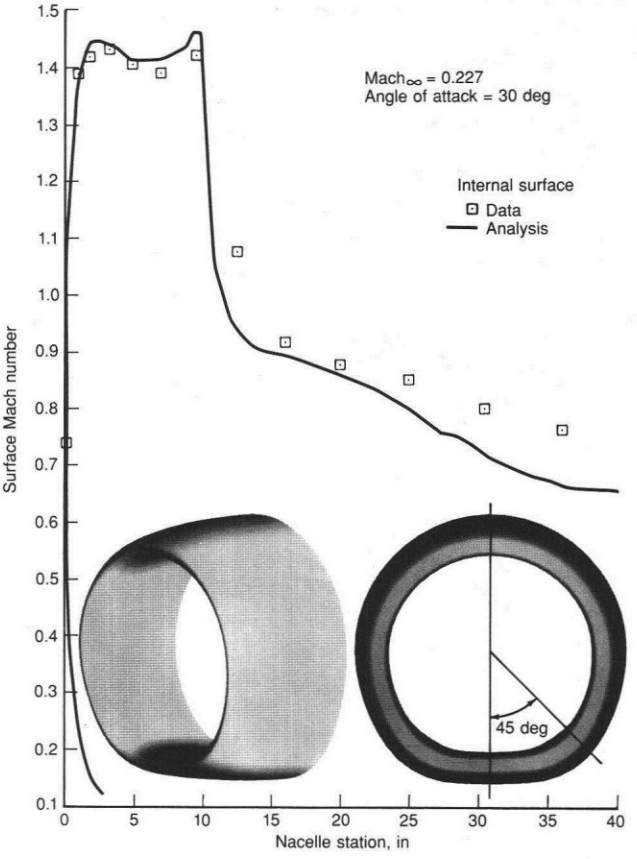

Figure 2. Comparison of Computed and Measured Inlet Surface Mach Number

The 3D boundary-layer program used in the analysis solves the compressible boundary-layer equations in curvilinear, orthogonal coordinates. This combination of procedures predicts inlet total pressure recovery with a high degree of accuracy and lip separation within ±1.5-deg angle of attack.

Supersonic Engine Inlets

Both inviscid and viscous techniques are applied to supersonic inlet design. The traditional analytical methodology described in the previous section does not apply here owing to the existence of strong shocks and the necessity to calculate through regions of separated flow. One computational method that has been applied to the problems discussed here is the U.S. Government-sponsored Reynolds-averaged Navier-Stokes/Euler code, PARC.[6]

Preliminary analysis of supersonic inlets is often performed inviscidly. This approach cost effectively defines shock structure and gives estimates of the surface pressure along the geometry walls. A selected portion of the grid used for an analysis of this type on a mixed-compression inlet is shown in figure 3.

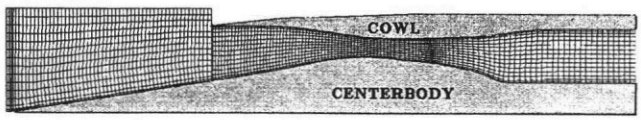

Figure 3. Grid System for a Mixed-Compression Supersonic Inlet

The Mach number contour plot presented in figure 4 shows that the predicted shock structure is as expected for the above geometry. This code is relatively insensitive to grid structure for this particular problem, and no mesh-adaptive routines have been incorporated.

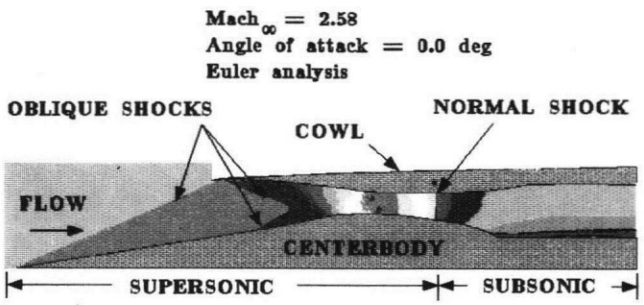

Figure 4. Geometry and Shock Structure Predicted by PARC2D for a Mixed-Compression Inlet

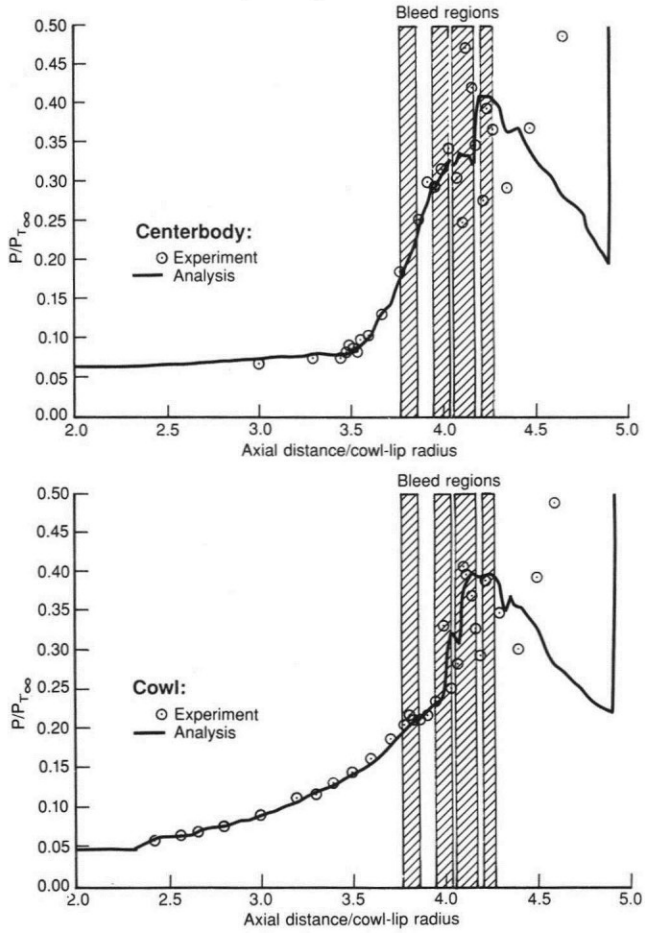

Figure 5. Comparison of Predicted and Measured Surface Pressure for a Mixed-Compression Supersonic Inlet

Wall-surface-pressure predictions are compared with experimental measurements in figure 5. The calculations and test results agree well except in the boundary-layer bleed region, where experimental data become erratic. As the inviscid calculations do not include this bleed, the predicted pressures are not expected to correlate well with test in this region.

The defining lines of a supersonic inlet with an open takeoff door are presented in figure 6 as an example of a viscous application of the code.

This door is necessary to provide increased airflow to the engine during takeoff as the inlet is sized for cruise conditions. Mach number and total-pressure contour results near the auxiliary intake are shown in figure 7. There appears to be boundary-layer separation on the forward surface of the auxiliary intake passage and subsequent reattachment before separation at the junction with the inner cowl, results that are considered plausible.

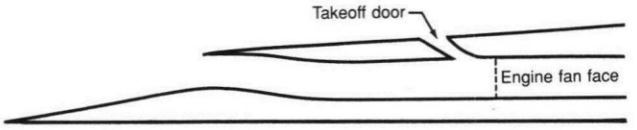

Figure 6. Supersonic Inlet With Takeoff Door

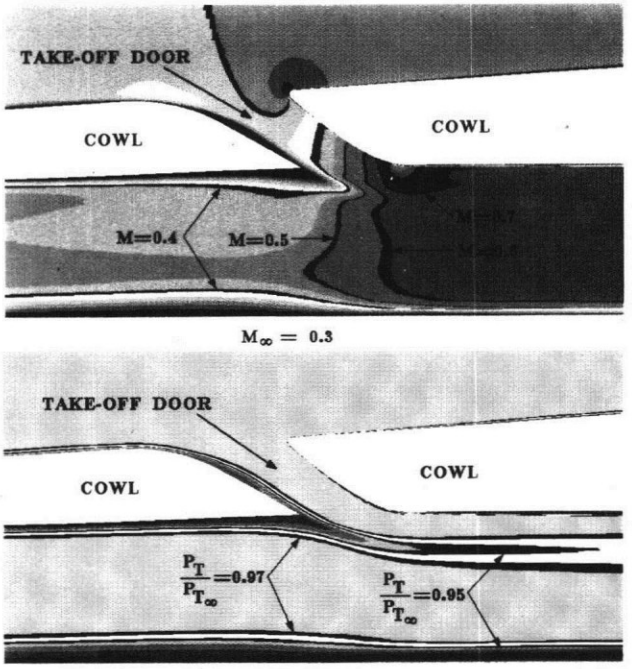

Figure 7. Axisymmetric Supersonic Inlet at Low Speed With Takeoff Door, Mach Number, and Total Pressure Contours

Exhaust Nozzles

The analysis of exhaust nozzles presents a particular challenge because of the complex physical nature of the flow, which is generally nonuniform in total pressure and temperature within and throughout multiple-turbulent-mixing streams and which may contain strong shock boundary-layer interactions. These conditions dictate use of a viscous formulation to analyze the problem. Again, PARC[6] is used to investigate these flows.

Most transonic transport aircraft engines possess nearly axisymmetric nacelles and aftbodies, which lend them naturally to axisymmetric analysis for the initial phase of isolated nozzle development. The design philosophy here is to minimize pressure variations between the duct walls to retard the development of secondary flows and to minimize the Mach number excursion from that of ideally expanded flow for a given pressure ratio. Along with the latter objective is the elimination or reduction in the strength of shocks. Figures 8 and 9 are examples of Mach number and surface-pressure results for a test geometry operating at high- and low-pressure-ratio conditions representative of cruise and descent engine-power settings respectively. Agreement between computational and experimental results is considered sufficient to use this procedure in engine-wing or engine-fuselage interference studies during aircraft preliminary design.

Once a configuration is developed based on the axisymmetric design process, the full 3D geometry may be analyzed using the 3D multiblock version of the code. This calculation provides an estimate of the losses associated with blockages, such as strut attachments or bifurcations, not modeled in the axisymmetric analysis.

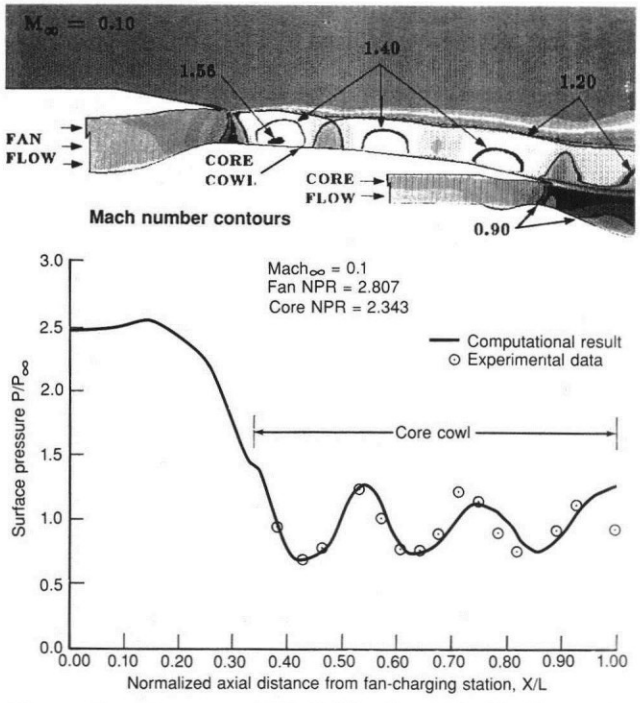

Figure 8. Computed Mach Number Distribution and Comparison of Predicted and Experimental Pressures Along Nozzle Core Cowl Surface

An example of Mach number results predicted by PARC3D is presented in figure 10.

One of the primary goals of the analysis is the prediction of nozzle performance (velocity coefficient, C_v) for a given design. An accurate value for this parameter is necessary to the computation of overall engine cycle efficiency and was, until recently, derived solely from experiment. This is no longer necessarily the case. Figure 11 shows a correlation between experimental and numerically derived values of C_v for the geometry shown in figure 10.

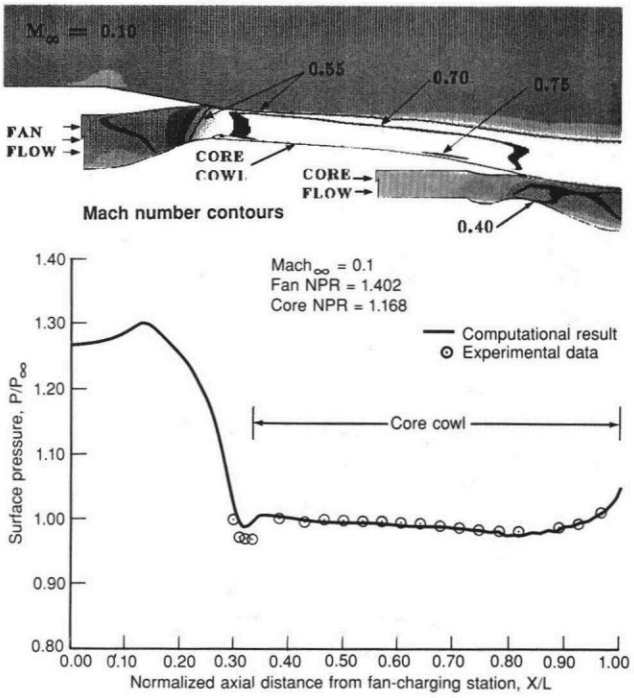

Figure 9. Computed Mach Number Distribution and Comparison of Predicted and Experimental Pressures Along Nozzle Core Cowl Surface

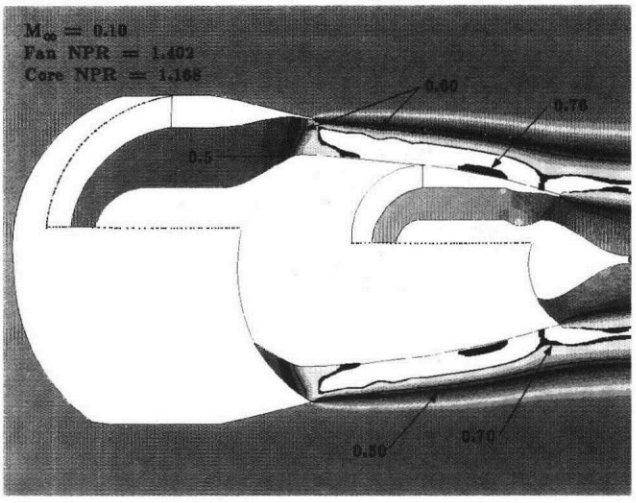

Figure 10. Mach Number Contours Resulting From a PARC3D Nozzle Flowfield Calculation

The trend of the analytical result tracks that of the experiment quite well. The difference in magnitude between the experimental data and the analytical results is on the order of 0.15%, quite good considering that parts of the test apparatus and their associated losses were not modeled.

A series of such curves can be created at various freestream conditions and used in conjunction with the local pressure field surrounding the installed nacelle (the computation of which is detailed in a following section) to estimate installed nozzle performance.

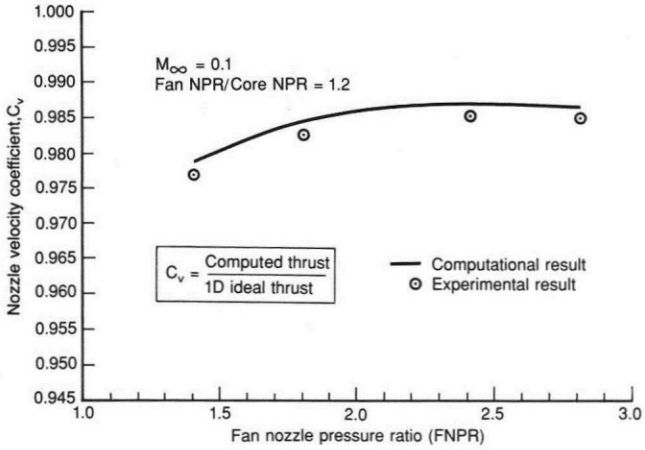

Figure 11. Comparison of Predicted Nozzle Velocity Coefficient, C_v, With Experimental Data

Another nozzle design issue that can be addressed by CFD is noise generation. Noise limit levels are becoming more stringent in the United States and abroad, leading to stricter design requirements. CFD is used in concert with noise analyses to correlate sound sources and pressure levels and, through an iterative procedure, is used to make appropriate geometry modifications to meet the required levels. Accurate predictions of field pressures are paramount to the success of this procedure. Figure 12 presents computed Mach number and surface-pressure results for a proposed supersonic transport mixer nozzle that is designed to abate exhaust noise by blending hot primary and relatively cool bypass streams.

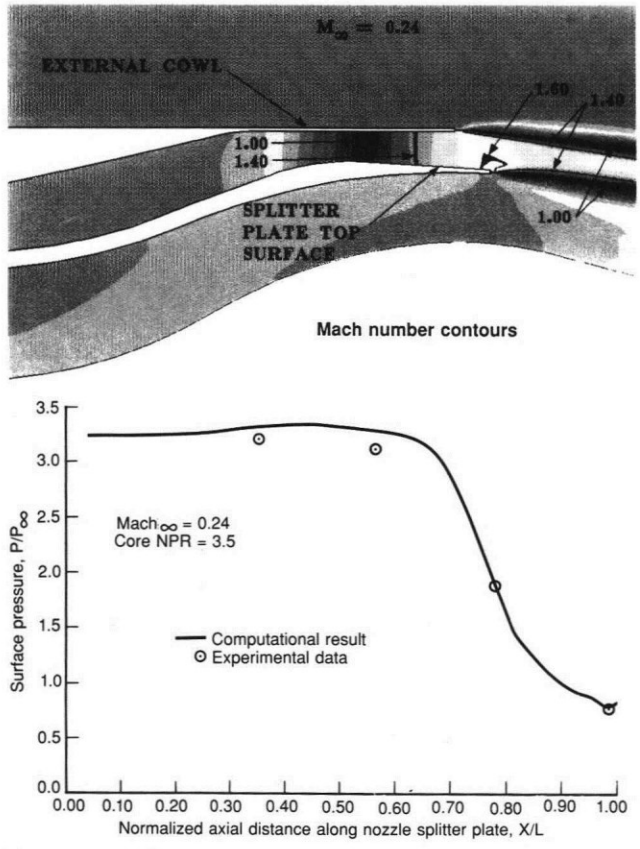

Figure 12. Computed Mach Number Distribution and Comparison of Predicted and Experimental Pressures Along Nozzle Splitter Plate Top Surface

Thrust Reversers

Modern high-bypass-ratio turbofan engines employ complex thrust-reversing mechanisms that pose significant challenges to design and analysis. The flow is strongly three dimensional, highly turbulent, and geometrically complex. Designers historically have relied heavily on model testing for both isolated and installed thrust reversers. Analysis can be used to address fundamental qualitative questions concerning issues such as flow separation around the reverser bullnose, effectiveness of the turning vanes of a cascade design, and general plume dimensions.

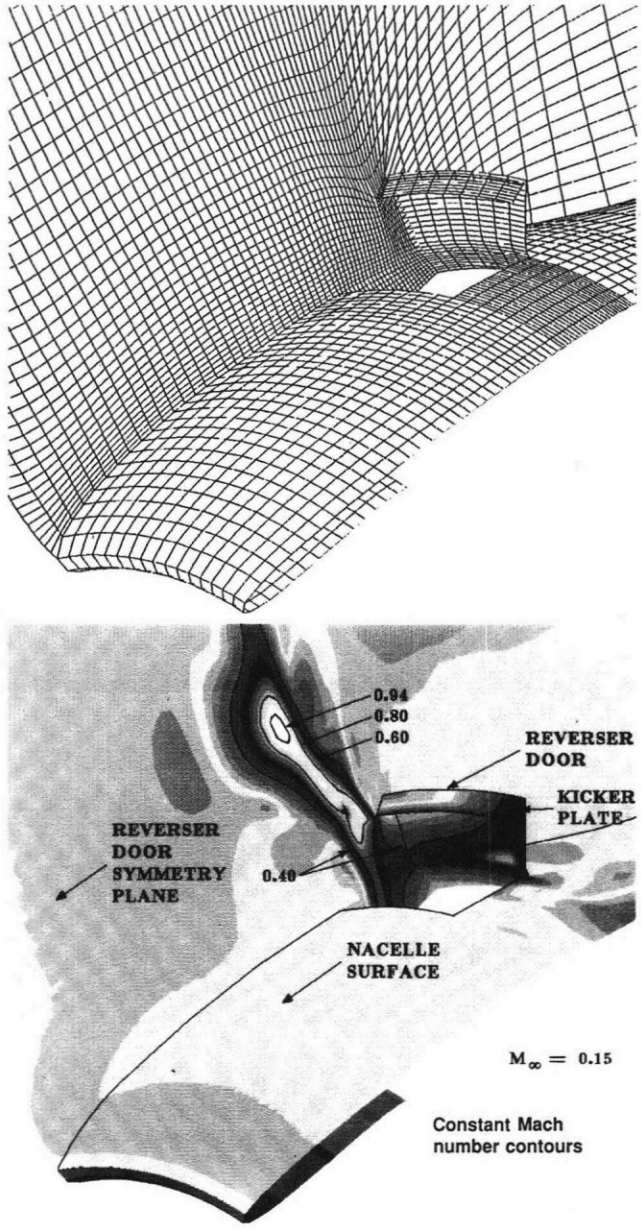

Figure 13. Example of a Grid and Results of a 3D Euler Calculation of a Four-Door Thrust Reverser Flowfield

Figure 13 presents, as an example, the mesh layout and results of a 3D Euler[7] calculation of a generic, isolated-four-door reverser operating at an external Mach number of 0.15. Results such as these are used to determine efflux patterns as an aid to door placement on the installed engine.

Figure 14 presents Mach number results, generated by a Navier-Stokes code[8], about an advanced, ducted, propfan engine reversing thrust via fanblade pitch reversal. In this particular case, interest was focused on the ability of the flow to navigate the required intake turn through the translating inlet sleeve at the rear of the nacelle and on the possibility of core ingestion of the reversed flow. This code can be run explicitly to investigate transient phenomena or implicitly to speed convergence to a steady-state solution.

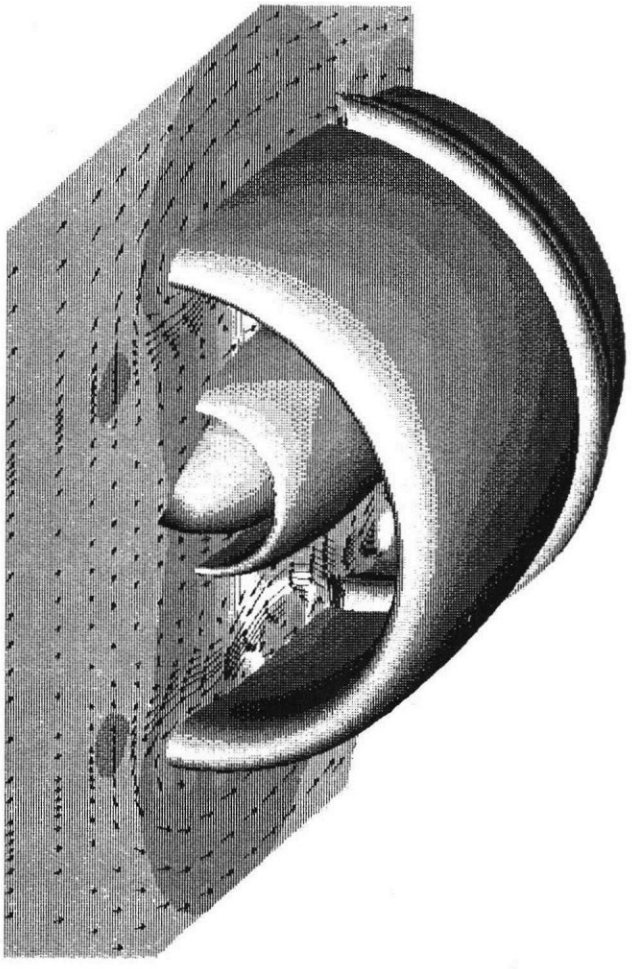

Figure 14. Investigation of Reversed-Flow Phenomenon of a Ducted Propfan Engine

Propulsion System Integration

Current large-diameter, high-bypass-ratio engines are closely coupled geometrically to the wing and body of subsonic transport aircraft in an attempt to avoid penalties associated with the aerodynamic isolation of the propulsion system. These penalties include the weight of longer landing gear and possible aggravation of wing flutter owing to increased pylon length. Improper integration of the propulsion system will result in a drag rise associated with the appearance of local regions of transonic flow in the area of the installation. This drag will grow to an unacceptable level above a given freestream Mach number, thereby limiting the cruise speed of the airplane.

Virtually all important features of subsonic transport installations can be investigated by using the Cartesian mesh, 3D transonic, full-potential flow code[1-4] described earlier. The code is valid for any application where the assumption of potential flow is supported, and it is able to handle a system of potential jump conditions trailing multiple lifting surfaces. Use of a Cartesian mesh as opposed to a body-fitted mesh substantially simplifies grid generation, eliminating analysis restrictions on complex configurations and saving time and expense. The mesh generation procedure is fully automated along with the determination of the coordinates and the surface normals of all intersects of the mesh and body required by the flow code. As in the analysis of subsonic inlets, the multigrid technique is employed for these complex configurations to aid convergence.

As an example of a Cartesian mesh applied to a propulsion installation, figure 15 shows an axial-plane cross section of a mesh through a nacelle, pylon, and wing geometry. This is a dense computational mesh that has adequate resolution for an actual propulsion installation application. Mesh stretching is used between the near field and the far field.

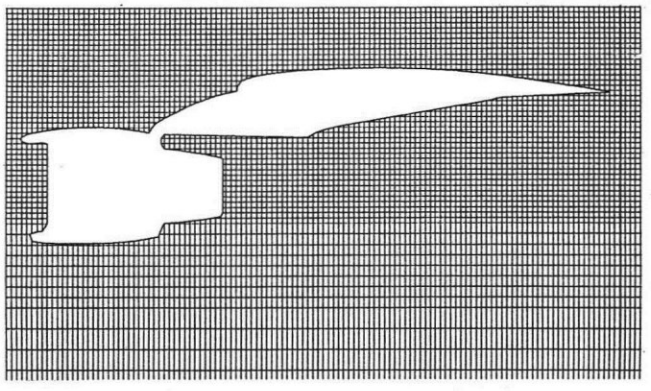

Figure 15. Typical Cartesian Mesh Plane Through a Wing-Pylon-Nacelle Geometry

The impressive capability of this code is demonstrated by comparing the analytical results to the experimental data presented for two configurations in reference 9. These two geometries consist of a body with clean-wing combination and the same body-wing configuration with a pylon-mounted long-duct nacelle. Three views of the body with clean-wing configuration are shown in figure 16. The nacelle configuration and its location on the wing (along with the location of the pressure taps) are shown in figure 17.

Figure 18 compares analytical calculations of Mach number on the undersurface of the wing for both the clean-wing and the pylon-mounted nacelle case (jet plume effects were not modeled, as flow nacelles were used in the test).

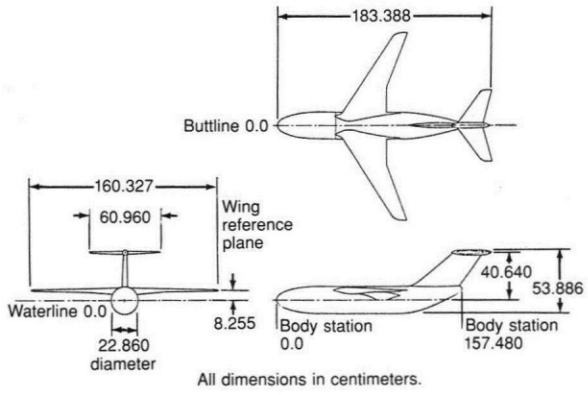

Figure 16. NASA High-Wing Transport—Clean-Wing Configuration

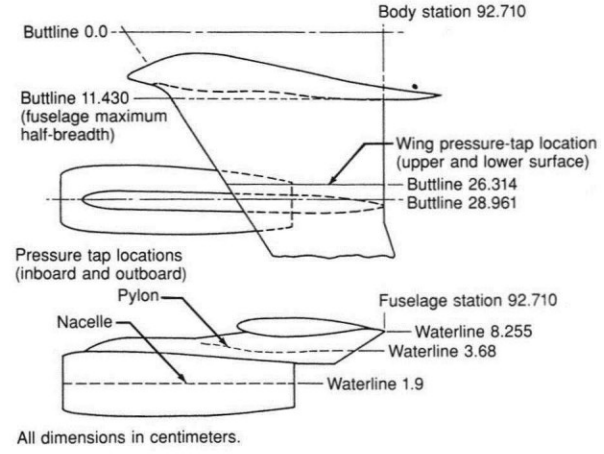

Figure 17. NASA High-Wing Transport Geometry and Instrumentation Locations for Wing, Pylon, and Nacelle

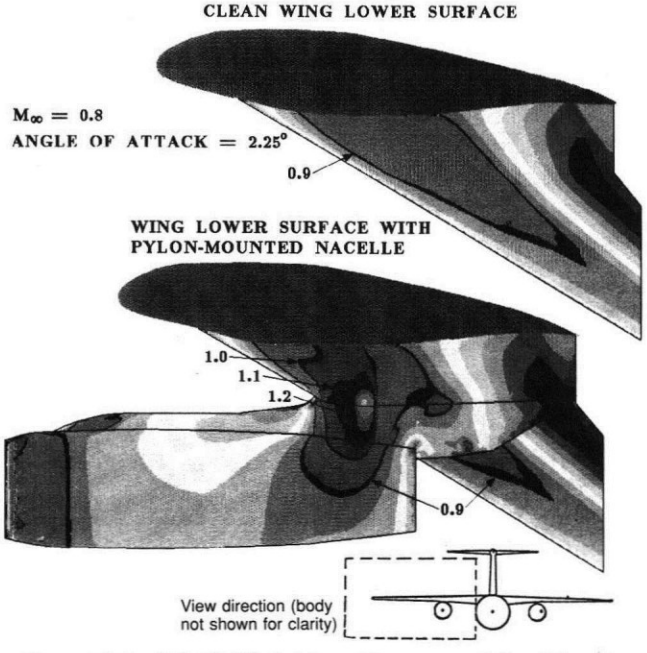

Figure 18. NASA High-Wing Transport, Wing-Nacelle Interaction—Mach Number Contours

The results show the effect that the nacelle-pylon installation has on the flowfield of the wing. Figures 19 and 20 compare these results to the experimental data in the form of pressure coefficient just inboard of the pylon position for the body with clean-wing and for the body, wing, pylon, and nacelle configurations respectively. Results for the body with clean-wing show a typical distribution for a supercritical wing section, with analysis and test data in good agreement. The addition of the pylon and nacelle (fig. 20) apparently causes a major change in the pressure distribution on the lower surface of the wing where a large region of supersonic flow appears followed by a shock at about the 30% chord location. Figure 21 shows a correspondingly high Mach number region on the pylon at about the same body station on the inboard side, while the outboard side remains subsonic. A similar comparison is made in figure 22 along inboard and outboard nacelle surface cuts. This figure shows that the external nacelle flow suffers in much the same way from the spillage-induced low-pressure regions at the leading edge of the cowl and further aft along the inboard nacelle surface.

This configuration clearly shows an inboard-side "channeling" effect caused by the location of the propulsion components on the wing that could easily lead to increased drag and reduced lift.

An additional concern with propulsion installations on subsonic transports is the interaction of the jet plume with the flow in the installed interaction region discussed previously. The plume can impose a pumping and blockage effect, making installation penalties worse. The most sophisticated approach to an investigation of this flow would use a Navier-Stokes analysis where most of the physics would be accurately modeled. The fact that the flow is not viscously dominated and shocks are relatively weak, taken with the high computation costs associated with mesh generation and flow-code computer time, directs that the methodology chosen be of a lower order.

An efficient method of simulating the plume has been devised involving an iterative procedure between the transonic potential code discussed previously and a jet plume model[10] that responds to local pressure variations predicted by the flow code. The procedure converges to steady state in three or four iterations.

Figure 23 shows calculated surface Mach number contours on the undersurface of the wing for a typical high-bypass turbofan engine installed on a twin-engine subsonic transport.

Figure 24 shows computed Mach number results for the wing upper and lower surfaces at a point just inboard of the nacelle in the interaction region.

The degree of interference for this case is indicated through comparison with the predicted lower surface Mach number distribution for the body with clean-wing configuration. Figure 25 compares the Mach number along the upper pylon location for a powered cruise case and a ram pressure ratio jet corresponding to a flow nacelle simulation. The Mach number spike at body station 880 appears to result entirely from jet plume effects.

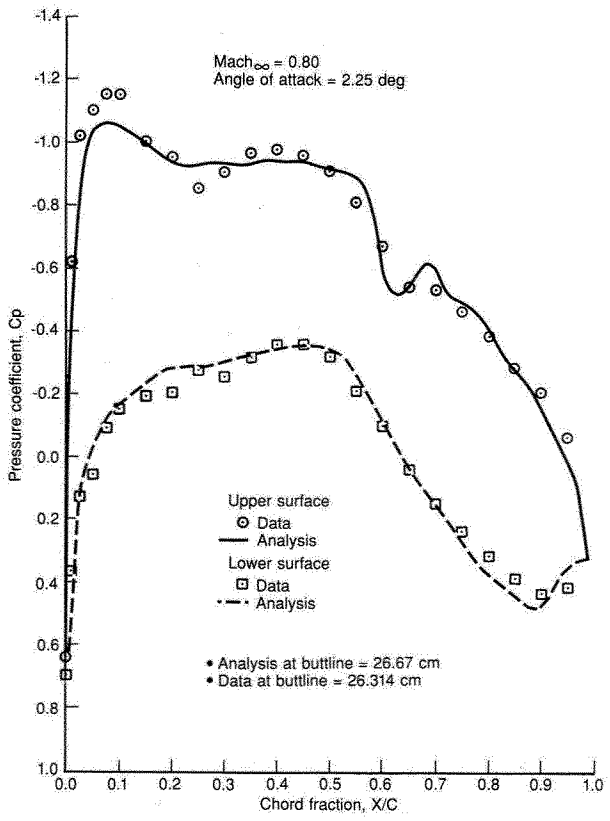

Figure 19. Comparison of Computed and Measured Pressure Distribution for NASA High-Wing Transport—Body and Clean Wing

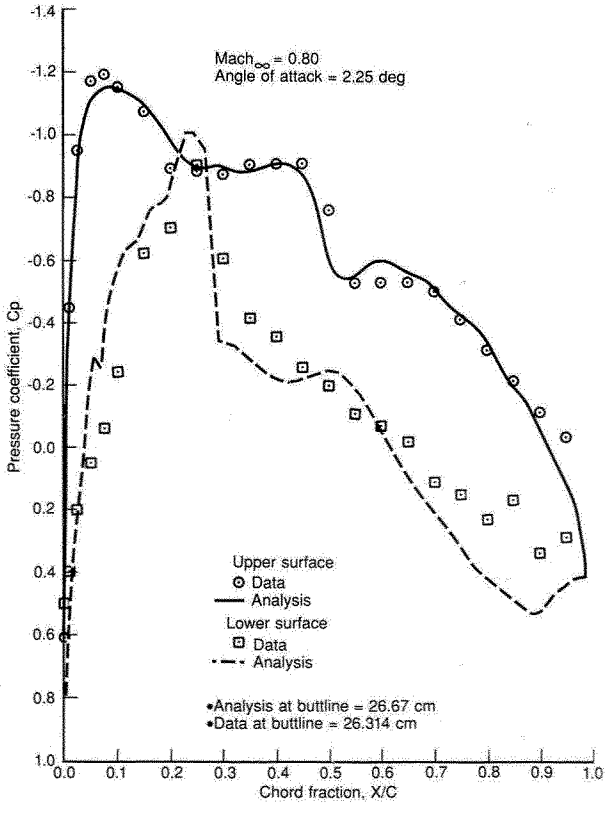

Figure 20. Comparison of Computed and Measured Pressure Distribution for NASA High-Wing Transport—Body, Wing, Pylon, and Nacelle

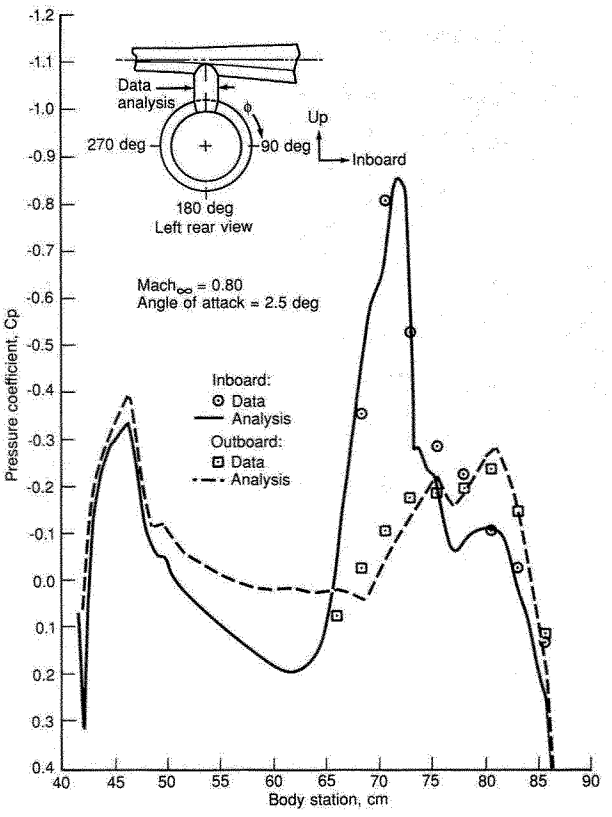

Figure 21. Comparison of Computed and Measured Pressure Distributions for NASA High-Wing Transport—Pylon

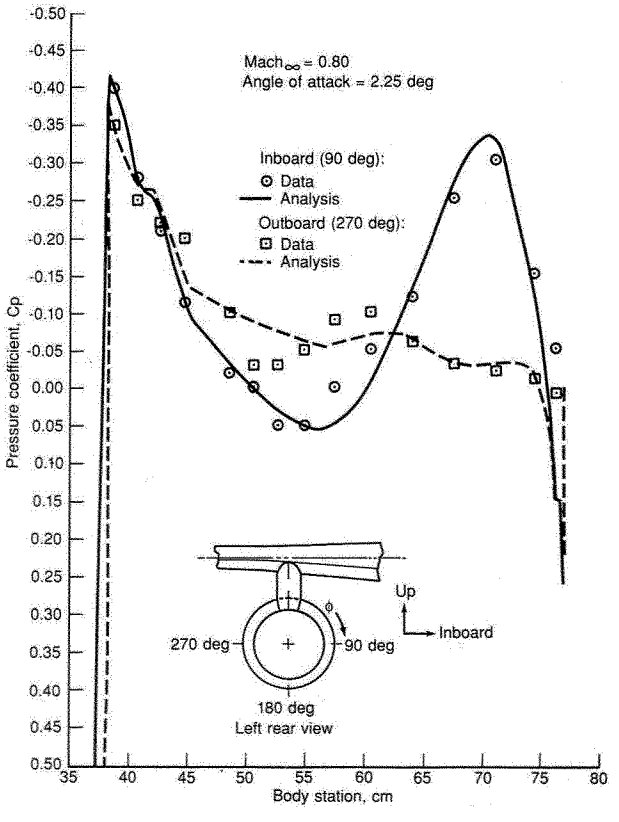

Figure 22. Comparison of Computed and Measured Pressure Distributions for NASA High-Wing Transport—Nacelle

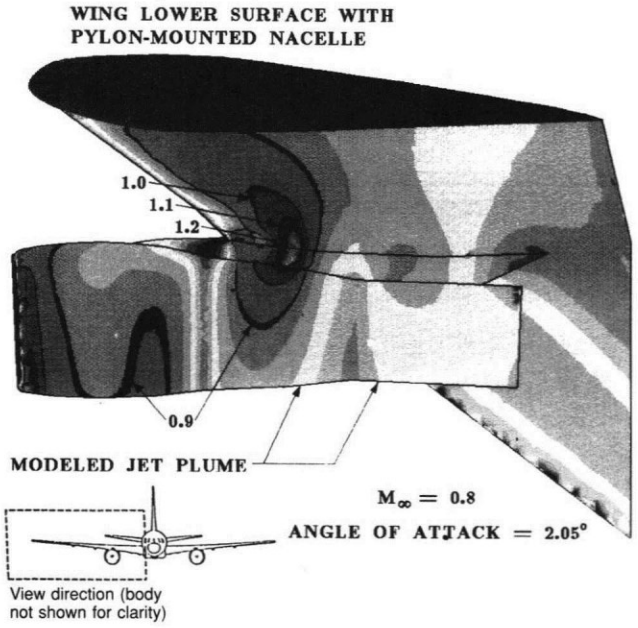

Figure 23. Nacelle-Wing Interaction With Plume Effects—Mach Number Contours

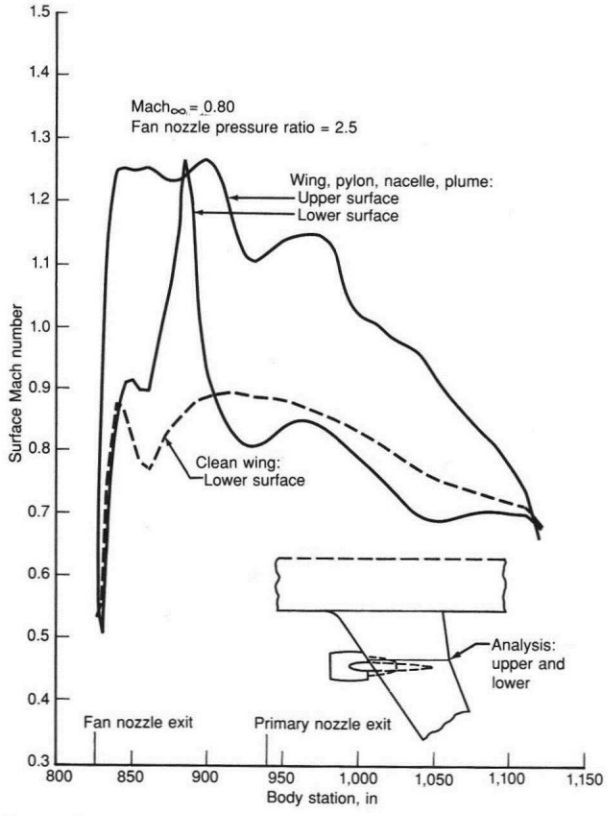

Figure 24. Comparison of Computed Wing Surface Mach Number With and Without Propulsion Installation Effects

Comparison of analysis with test data for both the potential flow and potential flow with plume model for other proprietary configurations has shown excellent agreement. This encourages confidence in their use as preliminary design

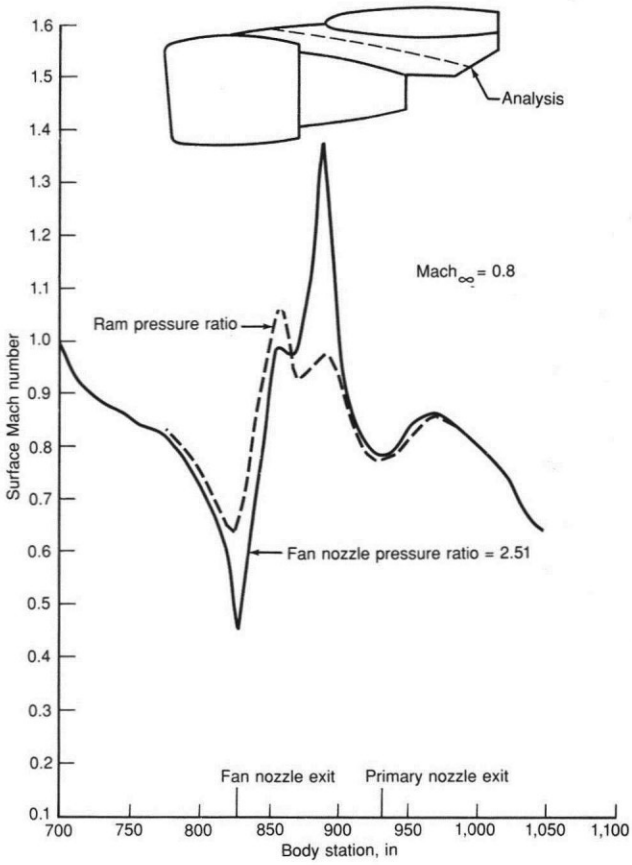

Figure 25. Comparison of Computed Pylon Surface Mach Number With and Without Jet Effect

tools to analytically study changes in pylon geometry and nacelle position to reduce adverse interactions.

Conclusion

Computational codes have been applied in propulsion system design at The Boeing Company for many years with great success. As a result of advancements in the sophistication of numerical algorithms and increases in computer size and speed, complex flow problems are now being analyzed successfully to improve aircraft performance. While great strides have been made, a continued effort is needed. It requires a significant investment in computers, skilled CFD analysts, and development of a database of test results for verification purposes.

The recent acquisition of a CRAY Y-MP and the continuing development of new codes maintains Boeing computational capability at the forefront of technology. Examples of the new codes on the immediate horizon include a full 3D interactive grid generator, which promises to greatly simplify current mesh-generation processes, and an Euler code with Cartesian/cylindrical mesh capability. The latter code will provide the same ease of mesh generation for complex geometries as the potential flow code discussed previously, but it will also allow for rotational flows and regions of differing total pressure and temperature to model nozzle plumes without iteration in propulsion system installation studies.

References

1. Reyhner, T. A., "Transonic Potential Flow Computation About Three-Dimensional Inlets, Ducts and Bodies," *AIAA Journal,* vol. 19, September 1981, pp. 1112-21.

2. Reyhner, T. A., "Computation of Transonic Potential Flow About Three-Dimensional Inlets, Ducts and Bodies," NASA CR-3514, March 1982.

3. Reyhner, T. A., "Three-Dimensional Transonic Potential Flow About Complex Three-Dimensional Configurations," NASA CR-3814, July 1984.

4. McCarthy, D. R., and Reyhner, T. A., "Multigrid Code for Three-Dimensional Transonic Potential Flow About Inlets," *AIAA Journal,* vol. 20, January 1982, pp. 45-50.

5. McLean, J. D., and Randall, J. L., "Computer Program to Calculate Three-Dimensional Boundary Layer Flows Over Wings With Wall Mass Transfer," NASA CR-3123, February 1979.

6. Cooper, G. K., "The PARC Code: Theory and Usage," Arnold Engineering Development Center, AEDC TR 87-24, October 1987.

7. McCarthy, D. R., and Foutch, D. W., "The Alternate Domain Coupling Procedure in CFD," published in the *Proceedings of the Eighth GAMM Conference on* Numerical Methods in Fluid Mechanics, September 1989.

8. Brown, J. J., "A Navier-Stokes Nozzle Analysis Technique," *Journal of Propulsion,* vol. 3, July-August 1987, pp. 334-41.

9. Lee, E. E., and Pendegraft, O. C., Jr., "Installation Effects of Long-Duct Pylon-Mounted Nacelle on a Twin-Jet Transport Model With Swept Supercritical Wing," NASA TP 2457, December 1985.

10. Colehour, J. L., Farquhar, B. W., and Reyhner, T. A., "Analytical Methods for Subsonic Propulsion System Integration," Ninth International Symposium on Air Breathing Engines, vol. 2, September 1989, pp. 1064-69.